Cosmetics for everyone requires testing for all ages: creation of 3D Bioprinted old and young skin models for real efficacy testing.

Lègues, Maxime[1]; Forraz, Nico[1]; Milet Clément[1]; Fera, Virginie[2]; Cassin, Florence[2]; Ponthier, Elise[2]; Laperdrix, Céline[2]; Ferrier, Wendy[1]; **McGuckin, Colin[1*];**

[1]CTISkin department, CTIBIOTECH, Lyon-Meyzieu, France; [2]Laboratoire Biologie Cutanee, YVES ROCHER, Issy-les-Moulineaux, France.

*Colin McGuckin, CTIBIOTECH, 5 Avenue Lionel Terray, Phone : +33 9 67 10 74 55, c.mcguckin@ctibiotech.com

Abstract

Background: Reconstructed skin has been studied for many years and keeps being improved for better physiological aspects. Although the complexification level of skin models increases with groundbreaking techniques, it remains essential to provide reliable and suitable tissue for cosmetics ingredients testing. Characteristic differences of skin ageing, barrier function, morphology or matrix protein expression, may significantly vary testing outcomes. We aimed here to create reliable single-donor 3D Bioprinted reconstructed skin, age-variable, in order to give predictable results in advanced cosmetic testing.

Methods: Human keratinocytes and fibroblasts were expanded from donors ranging from 1 to 67 years old. Low passage cells were mixed with suitable bio-ink, then cartridged into a pneumatic 3D bioprinting system and printed as full-thickness models. Younger donor models were, or not, treated with UV to mimic and induce natural skin ageing due to light exposure. Subsequent models were then harvested for histological analysis to evaluate structure and function of the models.

Results: Younger donors tended to mature faster and with a flatter less wrinkled surface. Significant response to UV exposure led to thinner and more cornified epidermis, constituting a suitable age-induced tool for damaged skin. By using a sacrificial bioprinting ink it was also possible to allow the formation of deeper wrinkle-like grooves seen in older skin.

Conclusion: It is now possible to select age-groups in efficacy testing which will allow for targeted product development *in vitro* to relate to *in vivo* final donor testing of cosmetics with better consideration of the human immunology involved.

1. Introduction.

The historical concentration of beauty marketing to the young and beautiful has thankfully given way to a broader fairer attention to women of all ages, and even men, with global cosmetics increasingly becoming a mainstream accepted globally. However, cosmetics for all ages is a challenge not to be underestimated. Young skin has significantly different characteristics to older skin. Thinning characteristics of older skin with changes in matrix protein glycosaminoglycan combinations, lower collagen and hyaluronic acid, damaged elastin and increased water loss from the barrier all lead to differences in how cosmetics react on older skin. The more sinusoidal nature of older skin in general and tendance towards wrinkles has important implications for how cosmetic ingredients are adsorbed to the skin. In addition, many of the OECD recommended tests are based on out of date manually constructed epidermal models, which, more often than not, contain pooled keratinocytes from many donors, with no regard for immunology at all.

For this reason, we have advanced our 3D bioprinted full thickness skin models towards creating a variety of age-related models, with same-donor cells (rare for *in vitro* skin models) to reproduce the level of thickness and sinusoidal behavior seen in real life with the aim to help advance efficacy testing.

2. Materials and Methods

2.1 Sample collection:

All cells used in this study were isolated from human skin samples following ethical consent. Skin samples, which were surgical waste, were transported under optimal conditions to ensure and maintain tissue viability. CTIBiotech is also certified by the French Ministry in charge of research for the preparation and conservation of elements derived from the human body.

2.2 Cell isolation:

Fibroblasts and Keratinocytes were isolated from human skin donors ranging from 1 year old to 67 years old, using enzymatic dissociation and grown in 6-well plates (Corning®) using RPMI 1640 medium (HyClone™, GE Healthcare) supplemented with 15% FBS (HyClone™), cyprofloxacin (4 µg/mL) and EpiLife® medium (Gibco™, ThermoFischer) supplemented with Human Keratinocytes Growth Supplement (HKGS, Gibco™) respectively.
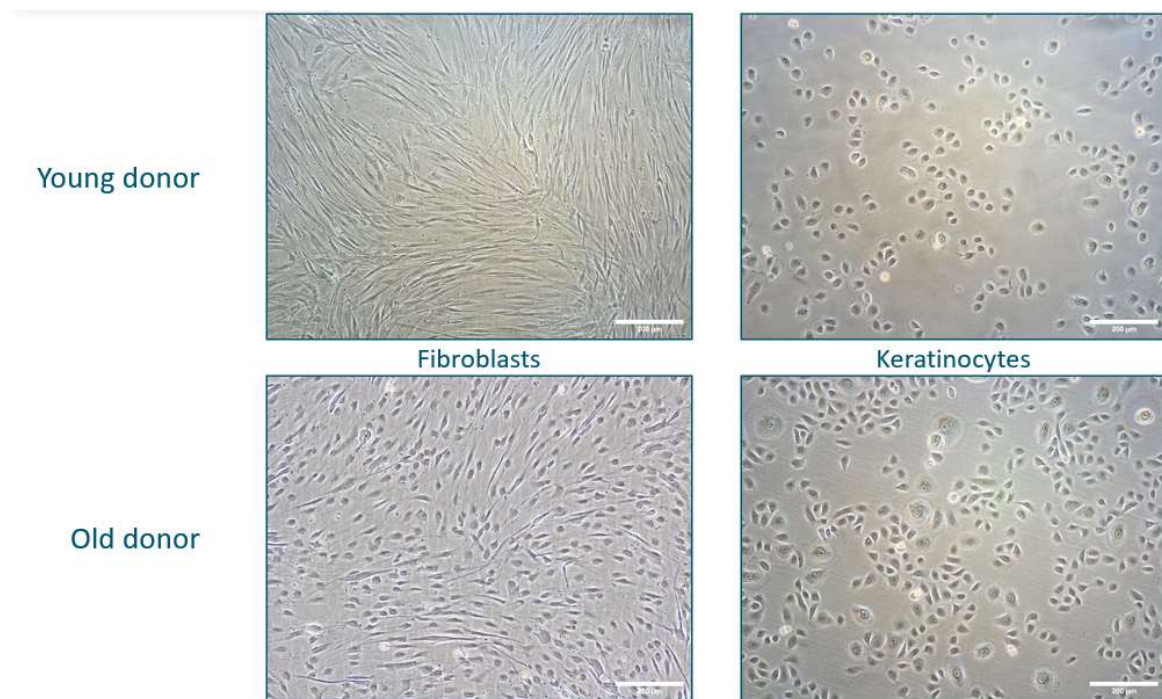

Figure 1., 2D cultures of human primary fibroblasts (left) and keratinocytes (right). Comparison between young (top) and old (below) donors.

2.3 Preparation of bioinks containing cells:

Under sterile conditions, cells at passage 2 or 3 were separately harvested, centrifuged, and counted. Afterwards, cells were resuspended with medium and transferred into 2.5 mL syringes before being mixed with skin bio-ink (CELLINK®, Sweden), into which epidermal adhesion proteins were added. Bioinks containing cells were then placed into 3 mL cartridges (Optimum® EFD, Nordson).

2.4. 3D Bioprinting:

The 3D model was designed using computer-aided design software. The 3D file was then converted to a G-code file using Slic3r software (as described at IFSCC2020, Henry Maso award 2022). Several infill patterns were applied (rectinilear, aligned rectilinear, honeycomb) with different infill percentage, from 20% to 40% (**Figure 2**.). Some 3D models were printed using a "sacrificial" ink, the Pluronic® F-127 (P2443, Sigma-Aldrich). The pluronic is a hydrogel, soluble in a cold solution. The powder was mixed with cold distilled water at a concentration of 30% (w/V), and agitated on ice during 1h30 before being sterilized by autoclave. The 3D models were printed including a pluronic layer, and rinsed with a solution of cold PBS 1X (Phosphate Buffered Saline 1X, Corning®) to eliminate the pluronic layer, in order to create grooves in the 3D model. The Gcode were then transferred to an USB stick and connected to a Bio X™ 3D bio-printer (Cellink®, Sweden). The 3D bio-printing process was carried out in sterile conditions, under a laminar flow hood to avoid contaminations. Cartridges containing bio-inks were placed in the defined print heads, G-code was selected, and full thickness epidermal-dermal skin same-donor models were 3D printed in 12-well plates with additional or subtracted laminin and collagen substitution, according to CTIBiotech optimization protocols.

***Figure 2.**, 3D Printing designs with demonstration models to improve dermal-epidermal junction shape with rectilinear infill pattern (left) and Honeycomb infill pattern (right)*

2.5. Maturation of 3D bioprinted models:

Printed models were grown in Transwell® (Corning®, VWR™) culture inserts, for a maturation time including dermal maturation, epidermis differentiation, air-liquid interface and cornification steps of the bioprinted skin. Delayed epidermal maturation was investigated by promotion of the dermal-epidermal junction before airlifting the models for both models with younger and older donors.

| Day 1 | Day 8 | Day 15 | Day 22 |

Figure 3., *Follow up of 3D Skin models maturation over 22 days. Pictures taken with Android phone camera, macro view.*

Skin models become progressively opaque as cornification forms.

2.6. UV induction:

Printed models from younger donors were inducted with a UV-A light source device (CTIBiotech, Lyon, France) at an irradiation value of 10J/cm², every day during 5 days. Printed models were placed in sterile PBS 1X (Phosphate Buffered Saline 1X, Corning®) before each induction to avoid interaction of UV-A rays with the supplements present in the culture medium. After irradiation, fresh culture medium replaced the PBS 1X and 3D models were incubated again at 37°C, 5% CO_2 until the next day.

2.7. Histological stainings:

At the end of the experiment, 3D models were rinsed once with PBS 1X and fixed in formaldehyde 4% w/v (Sigma-Aldrich), before dehydration in alcohol crescent baths and clarification in xylene. Samples were then embedded in paraffin and sectioned into 5 μm thick slices. Hematoxylin, eosin and saffron stainings were performed on slides after a

rehydration process. Immunohistochemistry stainings were also completed against CD44, HAS1 or HAS2 receptors.

2.8. Microscopical observations:

Microscopic observations were performed with a DM2000 optical microscope (Leica, Germany), Leica DMLB fluorescence microscope controlled by image acquisition software (LAS v4.2) and fluorescence microscope (Eclipse TI, Nikon) connected to NIS-element software (Nikon).

3. Results.

3.1. Printing parameters:

Reproducible replicates of the models were successfully produced following the 3D bioprinting of the two cell types used in the study, from younger and older donors: keratinocytes for epidermis and fibroblasts for dermis. Thanks to 3D pneumatic extrusion-based printer, many replicates were 3D bioprinted within an hour (**Figure 1.**).

Development of a multilayered skin model required maturation and an air-liquid interface step to allow for epidermal differentiation and maturation.

3.2. Generation of age-dependant 3D Bioprinted reconstructed skin and UV-A induction:

Three different reconstructed skin models were compared, either from young donors, older donors or UV-A light exposed young donor in order to generate "old-induced" model. 3D bioprinted models from younger donors were exposed to UV-A light to demonstrate their response to UV stress induction, in comparison with younger and older donors 3D models (**Figure 4**.).

***Figure 4**., Experimental plan for comparison of age-related 3D Bioprinted Skin model*

In older donor models (where no UV induction was performed), the fibroblasts grew well in the dermis, but the epidermis presented thinner differentiated layers, and a stratum corneum in formation. In younger donor models not exposed to UV-A light, the fibroblasts grew well too but the epidermis was thicker, with a better differentiation of the keratinocytes, from basal layer to stratum corneum. In the 3D "old-induced" models, UV light did not seem to have effects on the dermis structure, but significant effects appeared on the epidermis structure. Indeed, these models revealed a damaged and thinner epidermis after UV treatments, with anachronistic differentiation of the keratinocytes on the epidermis layers (**Figure 5**.).
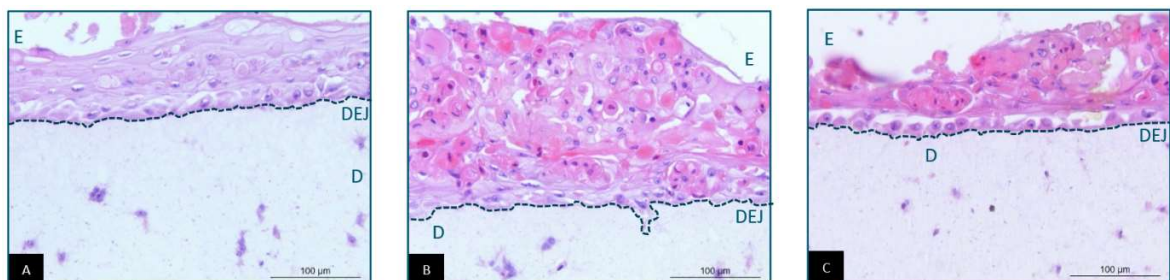

***Figure 5**., Histological analysis of 3D bioprinted skin models. Comparison between younger, older and UV inducted models.*
The structure of 3D bioprinted skin models was observed after Hematoxylin, Eosin, Saffron (HES) staining. A: 3D bioprinted skin model from young donor cells. B: 3D bioprinted skin model from old donor cells. C: 3D bioprinted skin model from young donor cells after UV induction. The D represents the Dermis, E represents the Epidermis, and DEJ is the

Dermo-Epidermic Junction. The pictures were taken with the Leica DM2000 optical microscope (x40).

3.3. Functional study of the 3D Bioprinted skin models

Although the structure of age-related (young, old, "old-induced") models was characterized after histological analysis, immunohistochemistry stainings were further performed on the models at the end of the maturation against CD44 receptors, HAS1 and HAS2 enzymes in order to confirm and better support the functional aspect of the 3D models (**Figure 6**.).
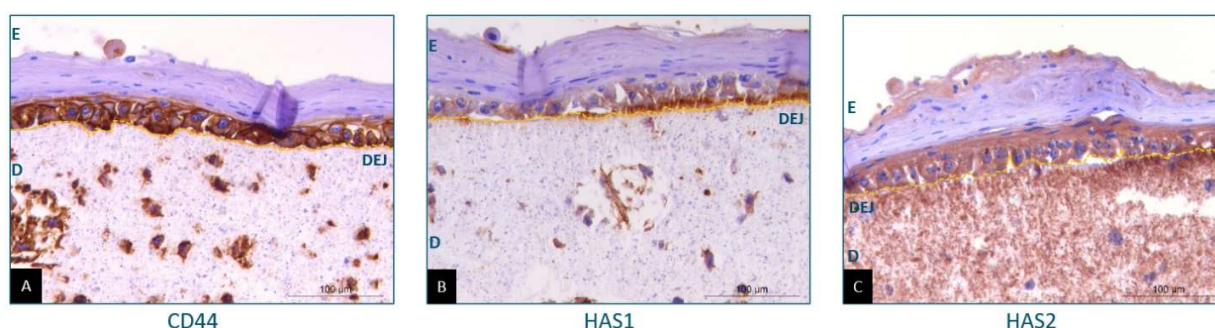

Figure 6., *Studies of 3D Bioprinted skin models regeneration capacity by histological analysis.*

Immunochemistry (IHC) stainings CD44 (A), HAS1 (B) or HAS2 (C) were performed on 3D Bioprinted models after maturation in order to highlight functionality of skin models. The D represents the Dermis, E represents the Epidermis, and DEJ highlights the Dermo-Epidermic Junction. Image acquisition by fluorescence microscope (Eclipse TI, Nikon) connected to NIS-element software (Nikon), x40.

Stained in brown (A), the expression of CD44 is mainly found in the epidermis (E). However, CD44 is not detected in the cornified layer. In a smaller amount, CD44 is also observed in the dermal part (D) of the bioprinted skin model. Stained in brown (B), the expression of HAS1 is found in the keratinocytes located in the epidermis (E), but also in the dermis (D). However, HAS1 was not detected in the cornified layer but seemed to be more expressed in the dermo-epidermal junction. Stained in brown (C), the expression of HAS2 is found in the keratinocytes located in the epidermis (E). Just like CD44 and HAS1, HAS2 was not detected in the cornified layer. In a smaller amount, some area in the dermal part (D) express HAS2.

3.4. Improvement dermal-epidermal junction sinusoidal shape:

3D Bioprinted Skin models optimized at CTIBiotech are functional models, but in order to optimized existing models, dermal-epidermal junction (DEJ) structure could be improved by enhancing sinusoidal shape to better mimic human skin physiology. In order to create such models with increased sinusoidal DEJ, several patterns were printed with demonstration ink to determine the best way to create such grooves (**Figure 2**.). Unfortunately, once bioprinted with the biological inks and cells, the resolution of the bioprinted models did not lead to significant differences in the structure of the DEJ compared to the previous models.

In an advance to that model, bio-printed models using sacrificial ink (pluronic) were thus developed. The DEJ formed in models printed with sacrificial ink increased the sinusoidal shape. It was also possible to observe sinusoidal shape in the dermal part, suggesting sacrificial ink and printing noozle dived into lower layers (**Figure 7**.).
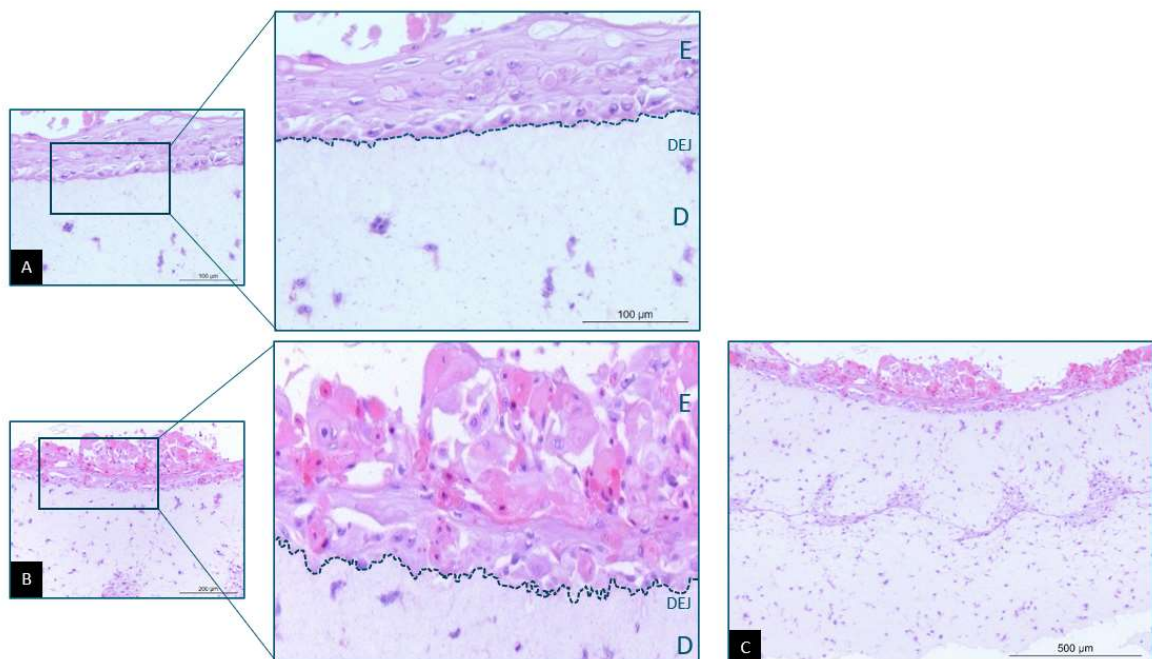

***Figure 7.**, Histological analysis of 3D bioprinted skin models. Comparison between flat models (A, x20) and 3D models printed with pluronic (B, x20 and C, x10). D = Dermis, E = Epidermis, and DEJ = Dermo-Epidermic Junction. Pictures were taken with the Leica DM2000 optical microscope.*

4. Discussion.

Fabricated skin models have historically tended to be quite flat with very little real-world bumps and inclusions. This has been a major draw back for real-world penetration kinetics and true efficacy testing. In our research we aimed to create models which created an overall structure allowing for a more real-world situation. Further a second major drawback of other manually available models is that in order to create 'off-the-shelf' tests, they are often derived from pooled donors which raises many immunological questions with regard to accuracy.

In our models, we are able to create both female and male models from same donor cell sources, so the immunology of these models can be considered more realistic in terms of safety testing, since the minor histocompatibility antigen system was not interfering in the same donor models. In addition, skin compositions vary according to internal and external factors (body location, genetic, age, UV stress) [4]. Biological advanced studies of human body, more specifically in skin, have helped our understanding that every skin does not react the same way to the same treatments. Thus, a higher diversification of cosmetic products has increasingly appeared, more specific to corresponding needs. In the same way, reconstructed skin models have to be physiologically more relevant and diverse to better assess the efficacy of active ingredients or cosmetic products. In this study, we compared histological properties of 3D Bioprinted reconstructed full-thickness models from same cell donor sources for both young and older cells ranging from 1 years old to 67 years old in order to propose adapted and representative tool for cosmetic industry.

3D bioprinting is widely used and diversify for skin reconstruction due to automation, accuracy, shaping, fidelity and high reproducibility [6,7,8]. Here, human primary amplified cells from both young and old donors were 3D bioprinted in a reproducible manner before maturation over more than 3 weeks (**Fig.3**). Whereas it was already possible to observe 2D morphological differences between human primary cells isolated from young versus older donor (**Fig.1**), histological analysis clearly highlighted discrepancy for both maturation and differentiation processes, especially for the epidermal layer (**Fig.5**). Furthermore, epidermal

reduction and higher cornification was noticed after photoaging due to UV stress stimulation shed light on model functionalization.

Hyaluronic acid or Hyaluronan (HA) is a key molecule in skin aging, involved in the skin regeneration and moisture [16]. Specific enzymes such as Hyaluronan synthase 1 (HAS1) or Hyaluronan synthase 2 (HAS2) are responsible for HA production. Consequently, HAS1 or HAS2 and CD44, a Hyaluronan receptor are reliable aging and functionalization markers of skin. Immunochemistry on 3D Bioprinted skin models revealed the expression of those 3 markers for young skin donor, offering a baseline level for aging characterization. Indeed, by measuring the expression gain of HA production on older skin model after treatment with cosmetic ingredient, it would be possible to point out the regenerative effects of new developed cosmetic product. Other biomarkers such as collagen (type I and III), fiber distribution, elastin and Fibrillin gene expression would be another alternative to better characterize ageing and photodamaged skin [12,13].

To reproduce the level of thickness and sinusoidal behavior seen in real life, modelling of 3D bioprinted models was investigated according to printing parameters, especially infill pattern and density (**Fig.2**). Although printing resolution has been incredibly improved over years regarding extrusion-based bioprinting, it is currently limited to 200-250 µm because of shear stress applied to human primary cells. Moreover, deposited bio-ink tends to fill the narrow-constructed grooves before firming up the printed after the crosslinking process. Another strategy was to involve sacrificial ink to support the printing construct during the crosslinking before simply washing the ink out and leave the desired grooves to reinforce the physiological non-linear aspect of dermal-epidermal junction. Compared to classical layer-by-layer deposit, sinusoidal shapes of about 250 µm has been observed diving into the dermis showing encouraging alternative to overcome technical printing resolutions limits (**Fig.6**).

Although there are technical limitations regarding printing resolution to obtain physiological repeated and reproducible ridges on 3D bioprinted skin, nevertheless, our study offers a good prospect for the improvement of existing 3D reconstructed skin models. Other on-going

strategies are currently being studied to better improve the sinusoidal aspect of the dermal-epidermal junction such as repeated stretching or shrinking processes.

5. Conclusion.

Improvement and diversification of 3D reconstructed skin models is a key to better assess safety and efficacy ingredient assessment. To personalize and propose a broader range of age-related skin models, we demonstrated the ability of our reconstructed skin models to develop according to age of donor. Furthermore, testing possibilities are even diversified with functional UV stress photoaging models. We demonstrated the functionality of models to synthesize Hyaluronan, a key marker involved in skin ageing, finally giving a great opportunity to the cosmetic industry to carefully assess next generation of manufactured ingredients.

Conflict of Interest Statement.
NONE.

References

1   Roig-Rosello E, Rousselle P. The human epidermal basement membrane: A shaped and cell instructive platform that aging slowly alters. Biomolecules. 2020;10(12):1-32.

2   Aumailley M. Laminins and interaction partners in the architecture of the basement membrane at the dermal-epidermal junction. Exp Dermatol. 2021;30(1):17-24.

3   Ciarletta P, Ben Amar M. Papillary networks in the dermal-epidermal junction of skin: A biomechanical model. Mech Res Commun. 2012;42:68-76.

4   Tobin DJ. Introduction to skin aging. J Tissue Viability. 2017;26(1):37-46.

5   Blackstone BN, Malara MM, Baumann ME, McFarland KL, Supp DM, Powell HM. Fractional CO_2 laser micropatterning of cell-seeded electrospun collagen scaffolds enables rete ridge formation in 3D engineered skin. Acta Biomater. 2020;102:287-297.

6   Lègues, M., Milet, C., Forraz, N., Berthelemy, N., Pain, S., André-Frei, V., Cadau, S., McGuckin, C. (2020). The World's First 3D Bioprinted Immune Skin Model Suitable for Screening Drugs and Ingredients for Normal and Inflamed Skin. IFSCC Magazine 4, 233-239

7   Lee V, Singh G, Trasatti JP, et al. Design and fabrication of human skin by three-dimensional bioprinting. Tissue Eng - Part C Methods. 2014;20(6):473-484.

8   Tarassoli SP, Jessop ZM, Al-Sabah A, et al. Skin tissue engineering using 3D bioprinting: An evolving research field. J Plast Reconstr Aesthetic Surg. 2018;71(5):615-623.

9   Rimann M, Bono E, Annaheim H, Bleisch M, Graf-Hausner U. Standardized 3D Bioprinting of Soft Tissue Models with Human Primary Cells. J Lab Autom. 2016;21(4):496-509.

10   Admane P, Gupta AC, Jois P, et al. Direct 3D bioprinted full-thickness skin constructs recapitulate regulatory signaling pathways and physiology of human skin. Bioprinting. 2019;15:e00051.

11   Qing C. The molecular biology in wound healing & non-healing wound. Chinese J Traumatol - English Ed. 2017;20(4):189-193.

12 Lovell CR, Smolenski KA, Duance VC, Light ND, Young S, Dyson M. Type I and III collagen content and fibre distribution in normal human skin during ageing. Br J Dermatol. 1987;117(4):419-428.

13 Bernstein EF, Chen QY, Tamai K, Shepley KS. Enhanced Elastin and Fibrillin Gene Expression in Chronically Photodamaged Skin. J Invest Dermatol. 1994;103:182-186.

14 Rittié L, Fisher GJ. UV-light-induced signal cascades and skin aging. Ageing Res Rev. 2002;1(4):705-720.

15 Contet-Audonneau JL, Jeanmaire C, Pauly G. A histological study of human wrinkle structures: Comparison between sun-exposed areas of the face, with or without wrinkles, and sun-protected areas. Br J Dermatol. 1999;140(6):1038-1047.

16 Papakonstantinou E, Roth M, Karakiulakis G. Hyaluronic acid: A key molecule in skin aging. Dermatoendocrinol. 2012;4(3):253-258.